Morphological modification of surface of crystal materials by means of ion-beam induced expansion

Sadao Momota
Kochi University of Technology

Contents

- Introduction
- Ion-beam (IB) technology applied to micro-nano scale fabrications
- Modification of crystal materials by means of IB-induced expansion
- Conclusions

Introduction

Precision of machining

Evolution of precision in machining process
- Most precise machining reaches atomic level.

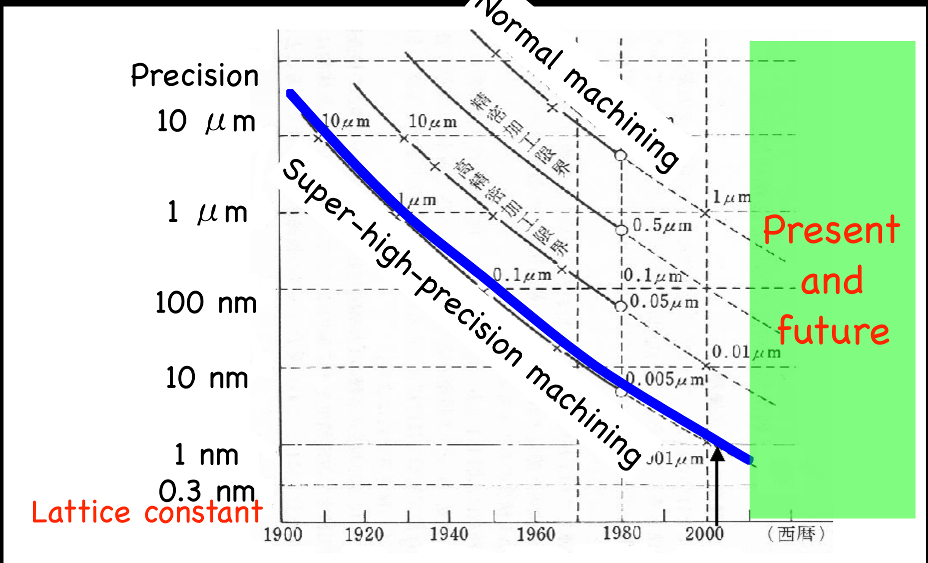

from Presentation by N. Taniguchi at ICPE

Miniaturization has stimulated a densification of fabricated structures.

Highly-integrated structures on material

Great success in micro-nano scale electronics

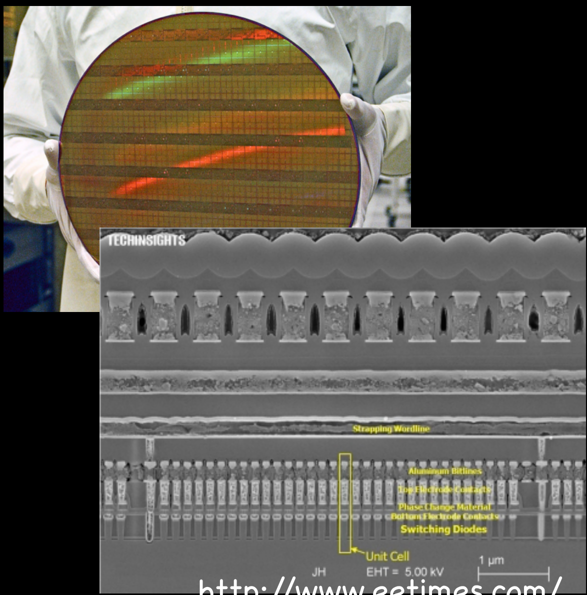

http://www.eetimes.com/

Cross-section of RAM
512-Mbit, Samsung

Conventional tech.

Electronic properties
Fabrication process :
Deposition
Lithography
...

dedicated to **2-dim** structures

At present,
Importance of **3-dim.** structures is increasing.

3D micro-nano structures

- MEMS
  Micro Electro Mechanical System
- Micro-machining tool
- Mold
- Optical device
- Biochip

3-Axis Accelerometer

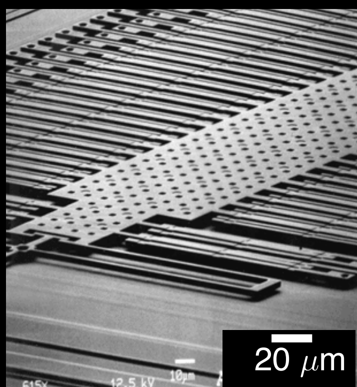

Analog Devices Co.
http://www.rise.waseda.ac.jp/proj/sci/S98S08/j-S98S08.html

Motion/deformation according to acting force

3D micro-nano structures

- MEMS
  Micro Electro Mechanical System
- Micro-machining tool
- Mold
- Optical device
- Biochip

Diamond array tool

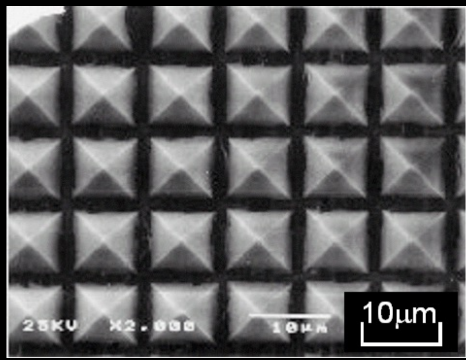

Morita Gr. (Toyama Univ.)

Small machining tools with high wear resistance

3D micro-nano structures

- MEMS
  Micro Electro Mechanical System
- Micro-machining tool
- Mold
- Optical device
- Biochip

Pattern transfer

SiO_2/Si → PMMA

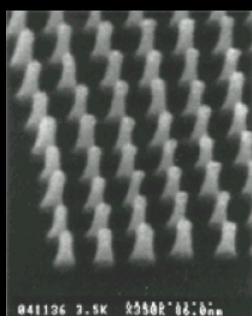

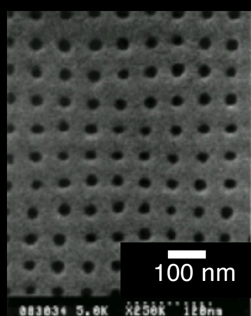

10nm diam. & 60nm pitch

S.Y. Chou et al.
J. Vac. Sci. Technol., B15(1997)2897

Mass production of structures with high aspect ratio

3D micro-nano structures

- MEMS
  Micro Electro Mechanical System
- Micro-machining tool
- Mold
- Optical device
- Biochip

Photonic crystal

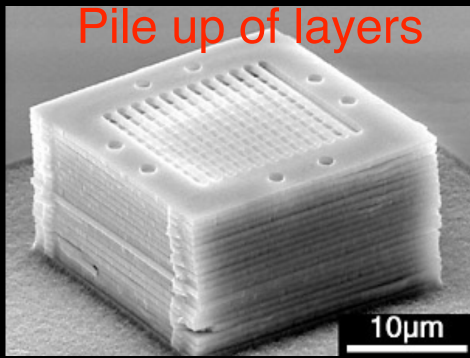

National Inst. for Material Science
http://www.nims.go.jp/jpn/news/nimsnow/Vol4/2004-03/05.html

Selective transmission of photon
wavelength, direction,
confinement, etc.

3D micro-nano structures

- MEMS
  Micro Electro Mechanical System
- Micro-machining tool
- Mold
- Optical device
- Biochip

Micro inspection chip

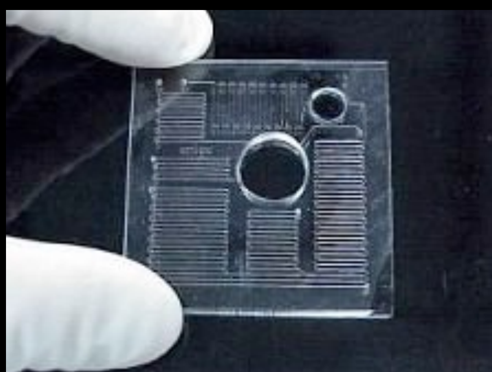

Hitachi, Ltd.

Medical inspection
in shorter time
with small amount of sample

Object of this talk

Structures in micro-nano meter scale

2D-structures / Single (electronic) function

→ **3D**-structures / **Mechanical** functions

Feasibility of IB-induced expansion effect :

- **Morphological** change
- **Mechanical** properties

In addition,

- Beam-material interactions
- Behaviors of defects

Beam-material interactions applied to fabrication processes

IB technologies in micro-nano fab.

IB-based fabrication processes

IB milling
IB deposition
IB lithography
Reactive ion etching

Basic processes

- Sputtering
- IB-induced damages …

AFM probe fabricated by FIB

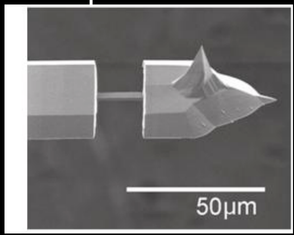

https://www.mecheng.osu.edu/pmcl/multi-axis-atomic-force-microscopy

Demonstration by FIB deposition/milling

http://fibics.com/Micromachining.html

Interaction between IB & materials

What would happen?

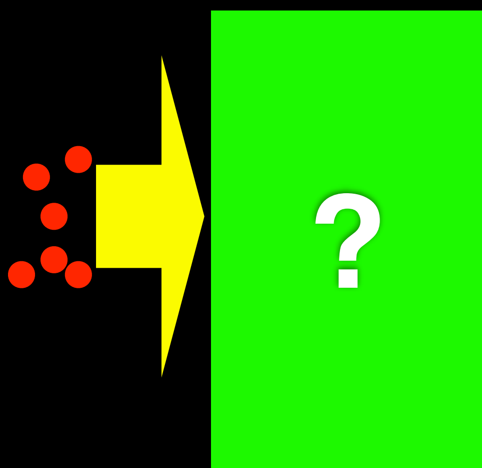

Interaction between IB & materials

- At surface :
  sputtering effect
  Removal of atoms
- Along trajectory :
  Production of defects
  Modification of lattice/chemical structures
- At final position
  Implantation of impurities

Specific depth of modified layer

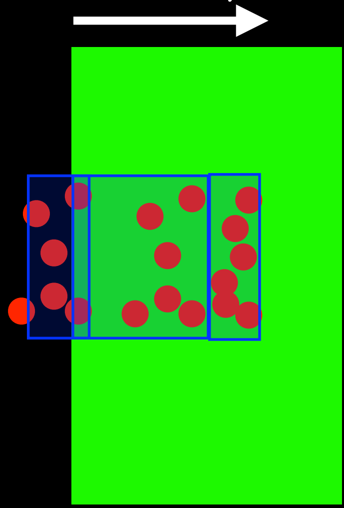

New possibilities of sputtering : 1

Sharpening or diamond knife

Profile of diamond stylus irradiated by Ar (1 keV)

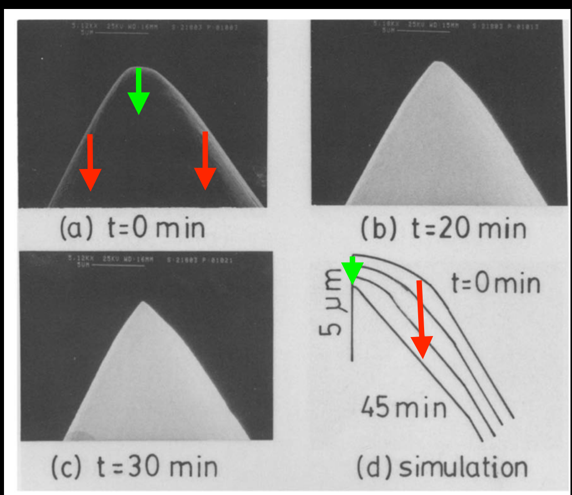

I. Miyamoto et al.
Nucl. Instr. Meth. Phys. Res., B39(1989)696

Based on

Angle-dependent sputtering rate

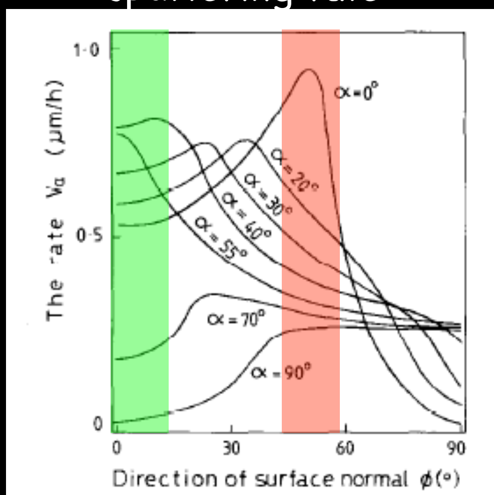

New possibilities of sputtering : 2

Wind patterns on surface

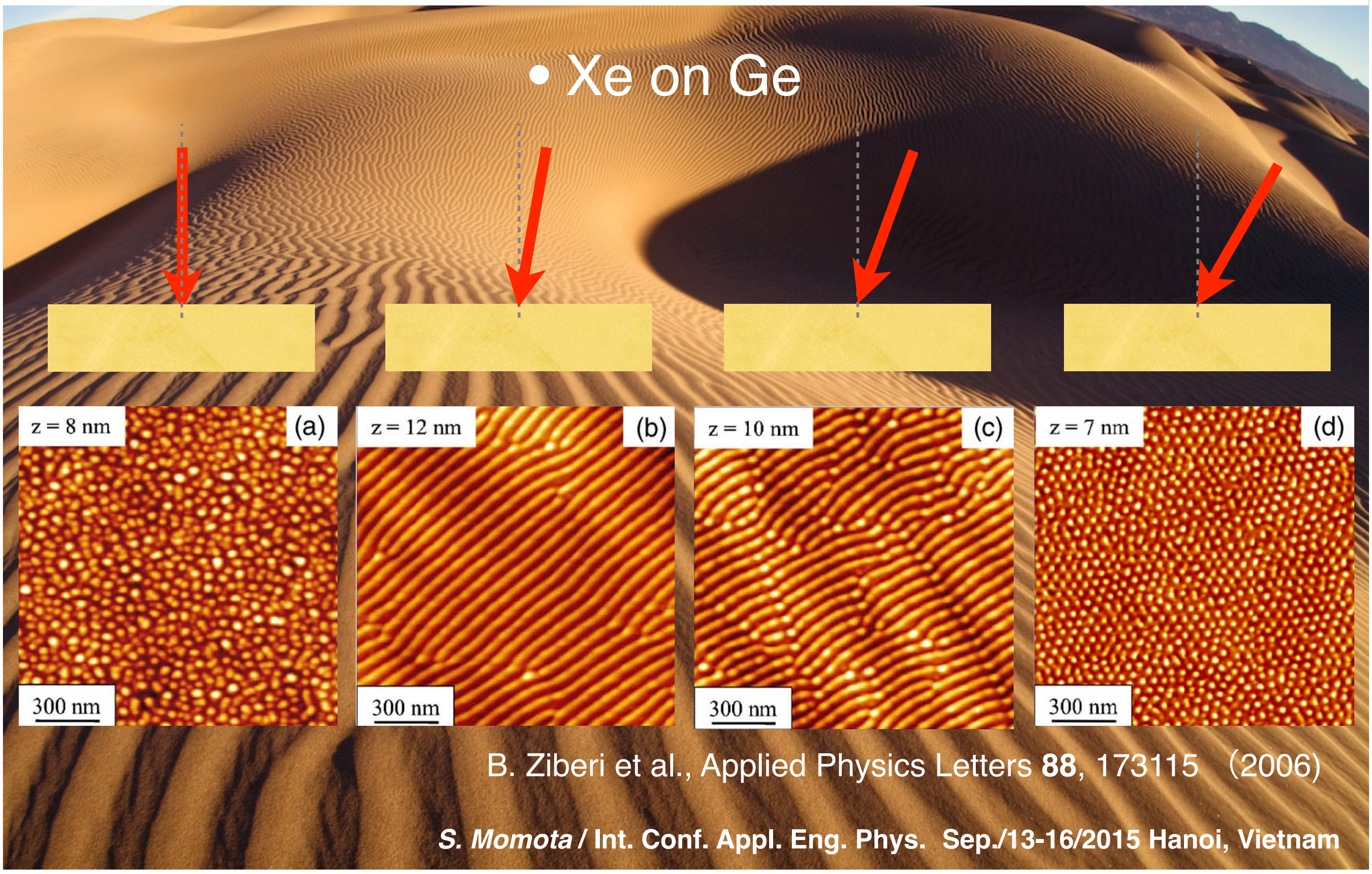

Lithography method

Projection of mask pattern

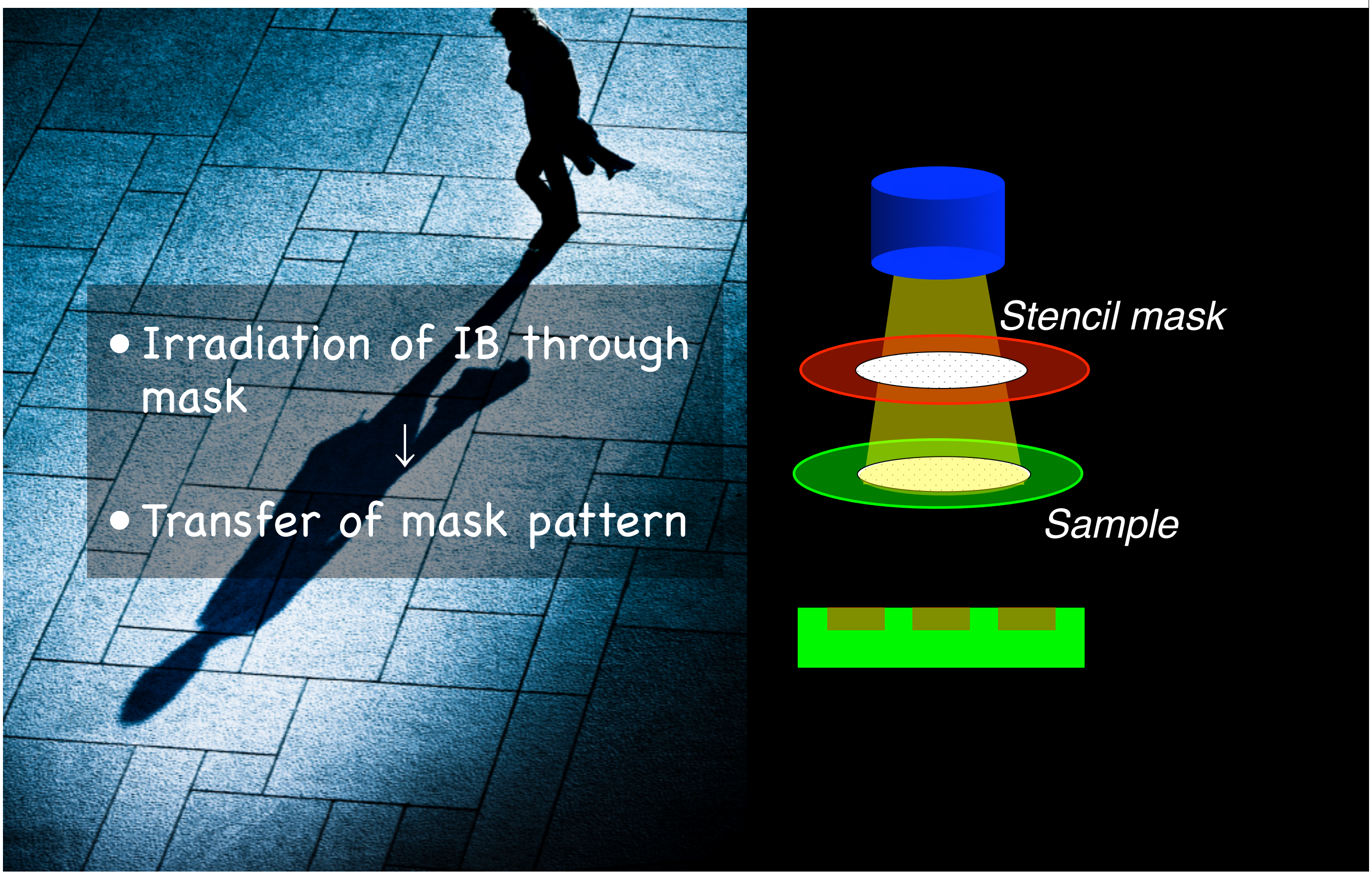

Fabrication by means of IB-lithography

2D-structures on Si-crystal

IB-induced defects -> Change in solubility against chemicals

1. Exposure : IB irradiation
2. Development : Etching in BHF solution

Ar^{4+} on Si

240 keV, 1.3x10^{15} ions/cm^2

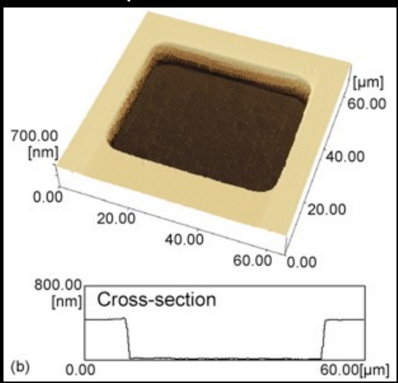

$T_{etch.}$ = 120 min.

Developed depth vs. beam energy

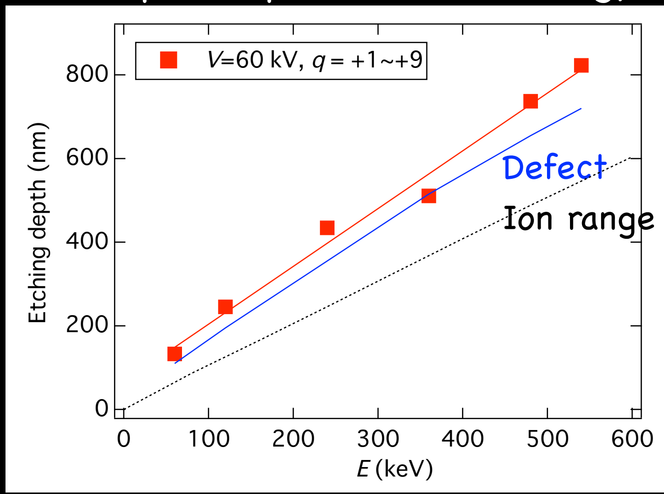

N. Kawasegi et al. Appl. Surf. Sci. 253 (2007) 3284.

Developed depth is determined by defect distribution.

S. Momota **/ Int. Conf. Appl. Eng. Phys. Sep./13-16/2015 Hanoi, Vietnam**

Modification of mech. properties

Mechanical properties of 6H-SiC irradiated by Au^{2+} (4MeV)

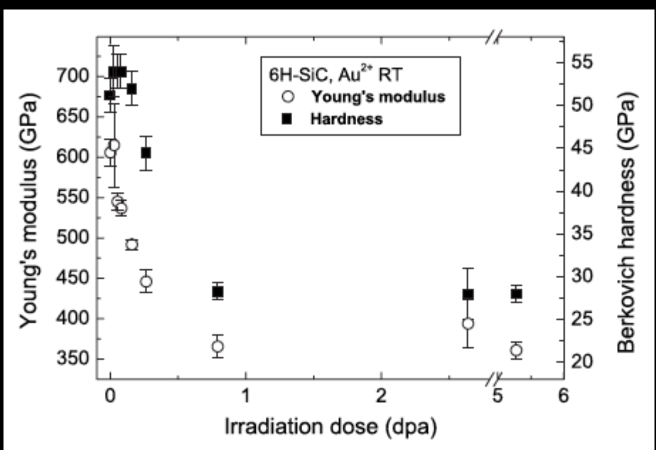

X. Kerbiriou et al.

J. Appl. Phys., 105 (2009) 073513.

Meas. at 200 nm (fixed)

R_p = 610 nm

Depth profile of disordered fraction

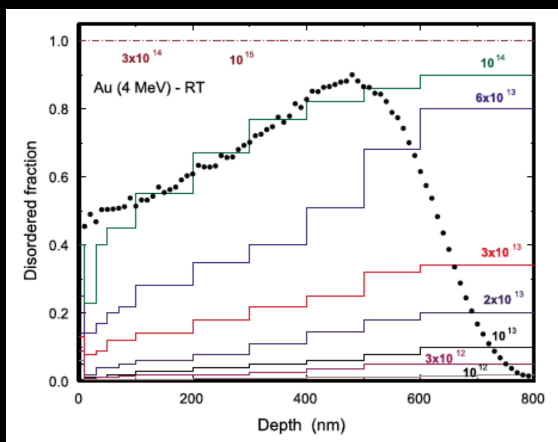

Modification of mech. properties should be depth-dependent.

However, few measurements.

S. Momota **/ Int. Conf. Appl. Eng. Phys. Sep./13-16/2015 Hanoi, Vietnam**

Advantages and limitations

Advantages	Limitations
High reactivity	Removal process
Controllability of depth	Time consuming
Small lateral struggling	Multi-step (lithography)

Features expected for processes to fabricate 3D structures

- Lower fluence
- Keep good mechanical properties
- Simple process

Ridge on cultivated field

Expansion induced by defects

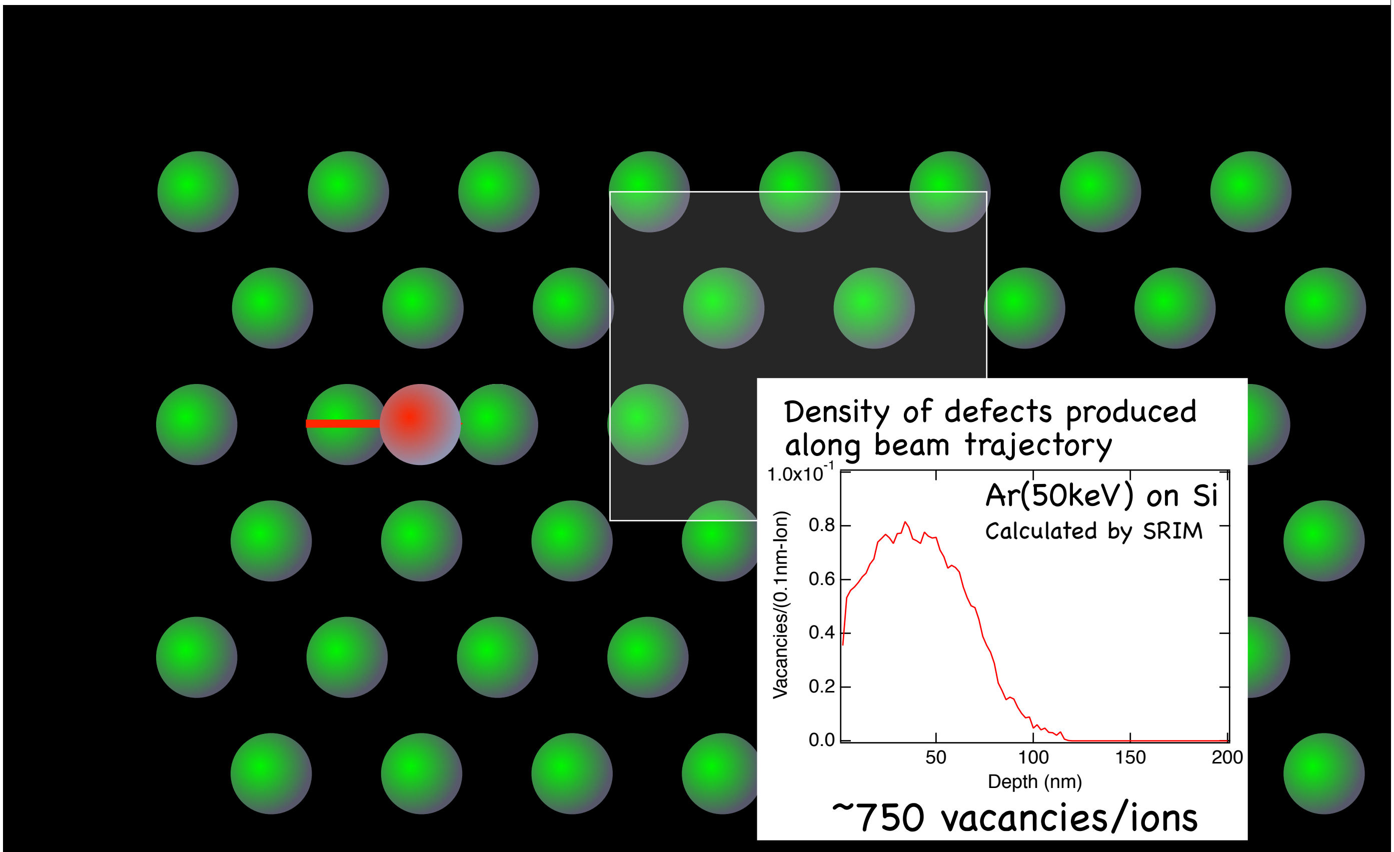

Step structure produced by Si-beam

Si (0.5~8 MeV) on (1 0 0) Si

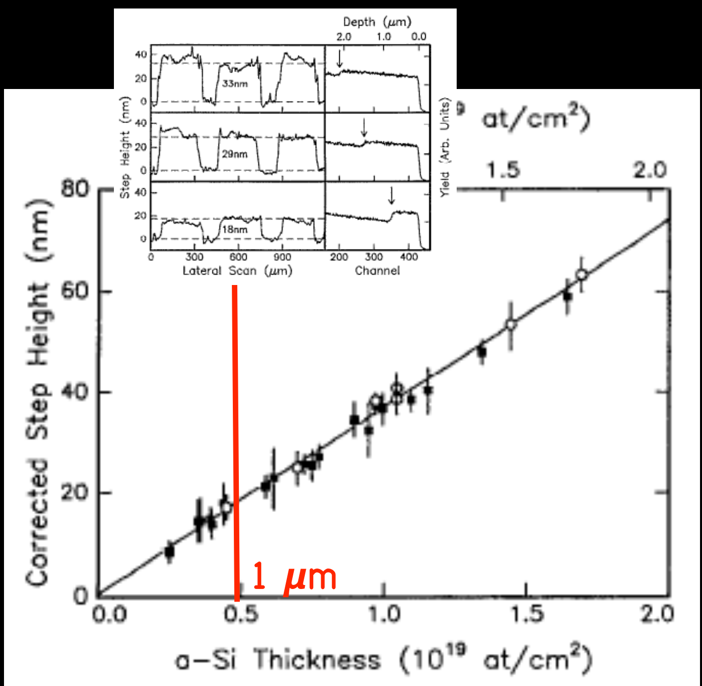

J.S. Custer et al., Appl. Phys. Lett. 64 (1994) 437.

n ~ 5×10^{15} /cm^2

Exp. rate = 1.8%

Observed expansion rate is
larger than that induced by implanted Si,
but, not so large.

Relaxation of defects
Immigration to surface
Recombination

Simulation of amorphization process

Molecular dynamics simulations.

Method	Relaxation	E_{dose} (eV)	V_{dose} (eV)	V/V_0	$E_{potential}$ (eV)
		EDIP			
100-eV irr.	z	6.5	10	1.036	-4.26
100-eV irr.	3D	6.5	2	1.035	-4.25
1-keV irr.	3D	6.5	3	1.022	-4.29
Variable *E* irr.[a]	3D	6.5	2	1.029	-4.26
Quench				1.035	-4.40
Variable *E* irr.[a]	900 K			1.036	-4.46
		T-III			
100-eV irr.	3D	8	12	1.095	-4.13
100-eV irr.	z	8	13	1.093	-4.13
1-keV irr.	3D	8	7	1.047	-4.20
1-keV irr.	z	8	13	1.045	-4.20
Variable *E* irr.[a]	3D	8	8	1.089	-4.13
Variable *E* irr.[b]	3D	11	11	1.08	-4.14
Quench				1.019	-4.40
		SW			
1-keV irr.	3D	17	17	0.947	-4.09
Quench				0.944	-4.11
Expt.		12[c]		1.018[d]	

J. Nord et al., Phys. Rev. B65 (2002) 165329.

Calculated with 3 potentials EDIP, T-III, SW

Calculated results show remarkable dependence on potentials and parameters.

Even sign changes.

Plastic deformation

a-Si pillars irradiated with 30MeV Cu, 8.2×10^{14} cm^2

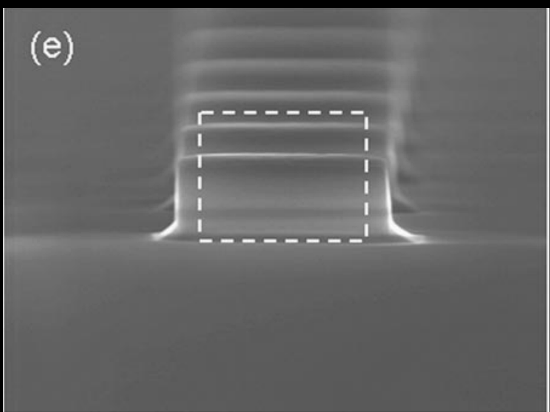

T. van Dillen et al.
Appl. Phys. Lett., 84 (2004) 3591.

Colloidal silica particle irradiated with 4 MeV Xe^{4+}, 4×10^{14} cm^2 at 85 K.

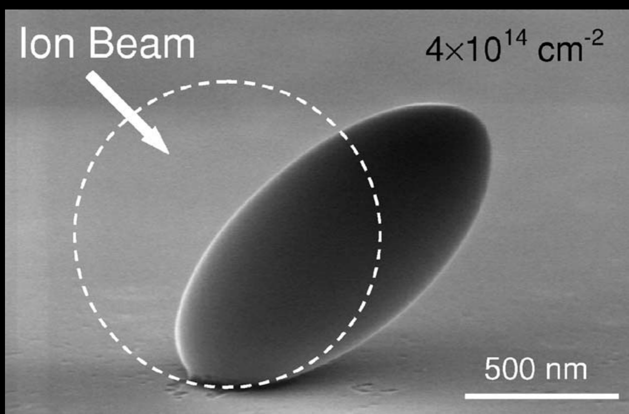

T. van Dillen et al.
Phys. Rev. B 74 (2006) 132103.

Anisotropic deformation has been observed.

Viscoelastic and free volume model
H. Trinkaus and A. I. Ryazanov, Phys. Rev. Lett. 74, 5072 1995.

Explained by IB-induced Newtonian viscous flow
described in the above reference

Modifications of crystal materials by means of IB-induced expansion

Ion-beam facility @KUT

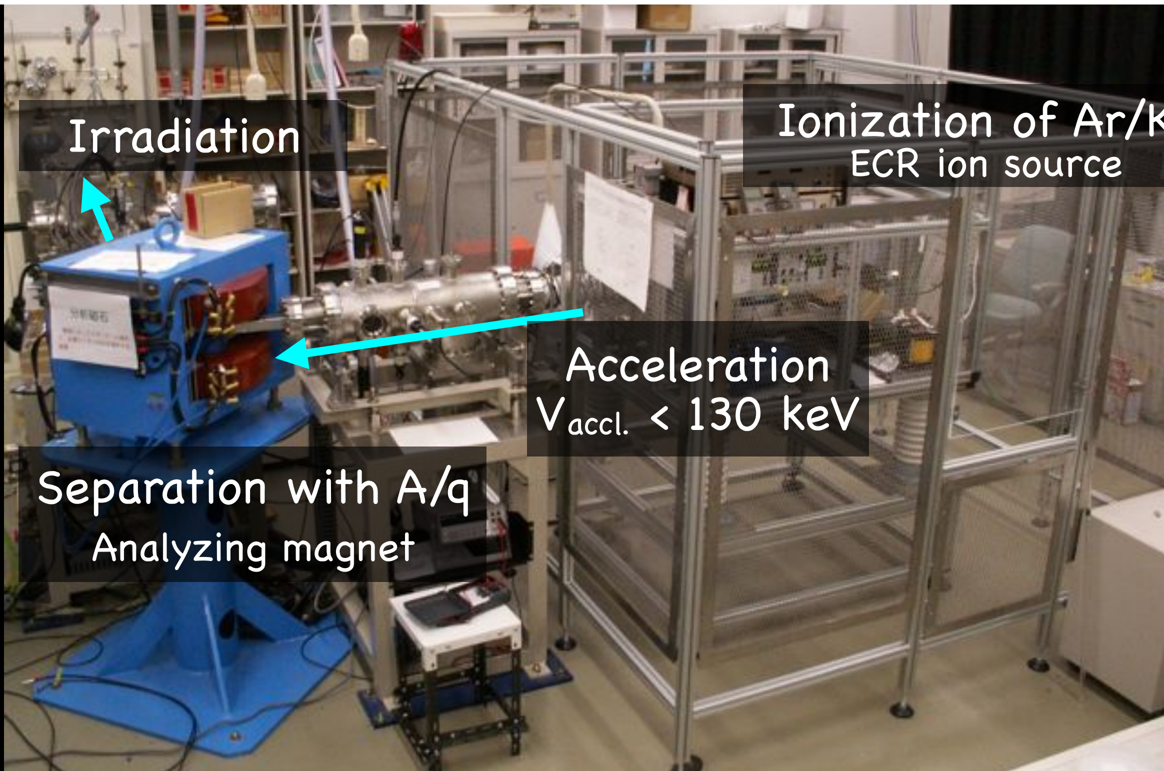

S. Momota et al., Rev.Sci.Instr. 75(2004) pp. 1497.

Highly-charged ions

High efficiency for beam acceleration

Kinetic energy : E = qeV

Ex. Ar on Si, V=100 kV

q	E (keV)	Range (nm)
1+	100	~100
10+	1000	~1000

Vertical deformation

Swelling height vs. fluence

C, Ar (90 keV) on (1 0 0) Si

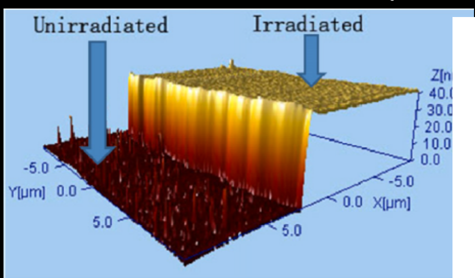

J. Zhang et al.
Nucl. Instr. Meth. Phys. Res., B282 (2012) 17.

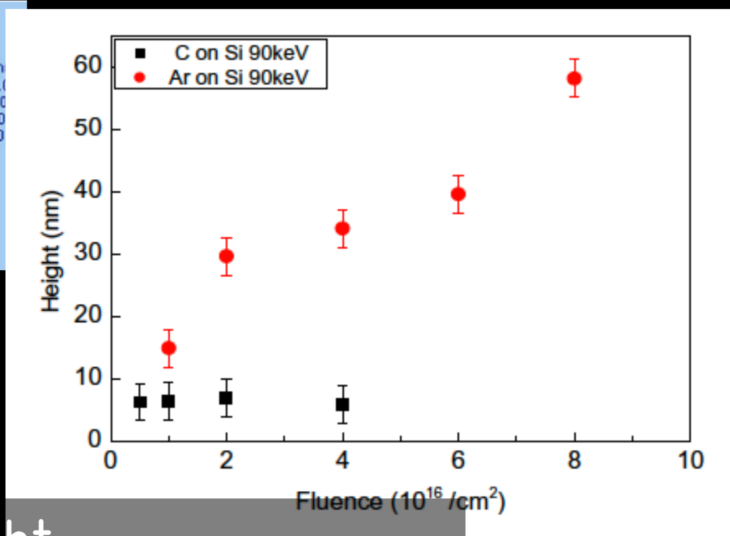

Obs. swelling height
- increase with fluence of Ar-beam.
- shows strong Z dependence.

Vertical deformation

Swelling height vs. energy

Ar on (1 0 0) Si

$n \sim 1.3\times10^{15}$ /cm^2

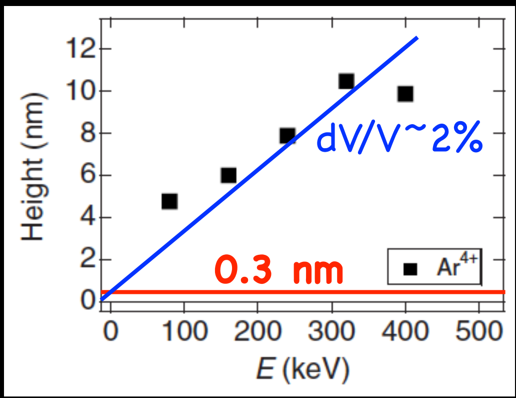

S. Momota et al.
Rev. Sci. Instrum. 79 (2008) 02C302.

E = 50, 240 keV

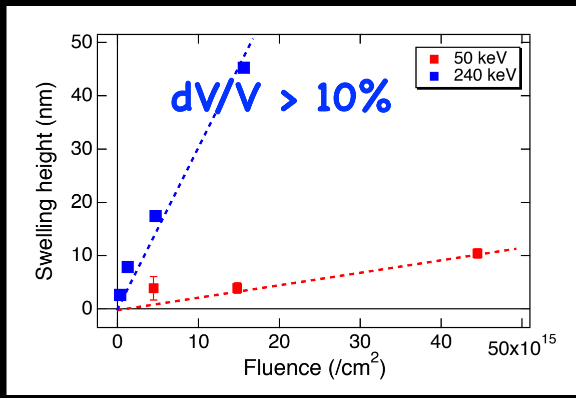

1. Obs. swelling height increase with R_p (E).
2. Minor contribution of implanted Ar.

Contribution of IB-induced defects

Vertical deformation

Molecular dynamics (MD) simulation

Evolution of Si-lattice system simulated by MD

S. Satake et al. J. Appl. Phys. 106 (2009) 044910.

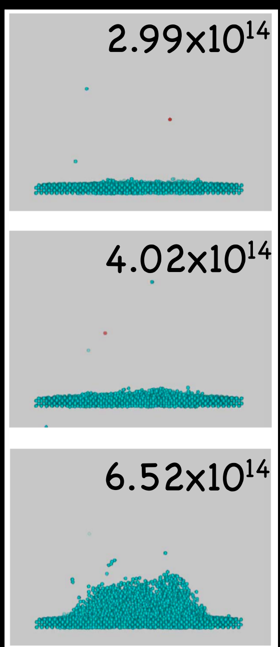

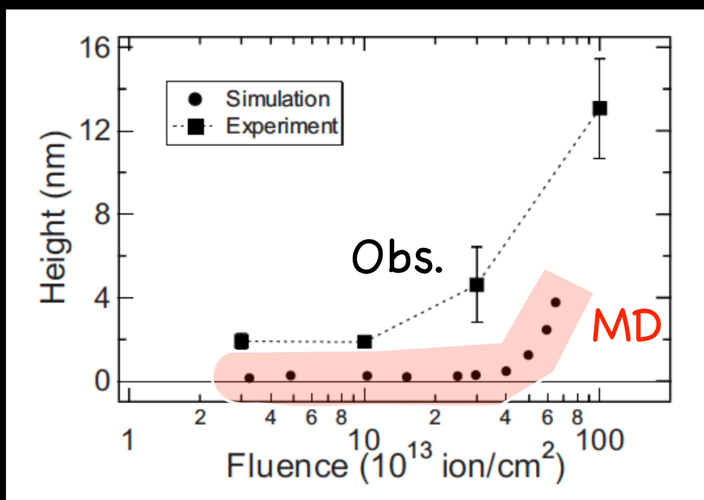

Fluence dependence is roughly OK.
But, underestimate in absolute values.

Lateral deformation

Deformation observed by SEM

Kr (240 keV) on c-Si with stripe structures

n ~ 8×10^{13} /cm^2

X. Guo et al., e-J. Surf. Sci. Nanotech. 13 (2015) 35.

Top view of line and space structure

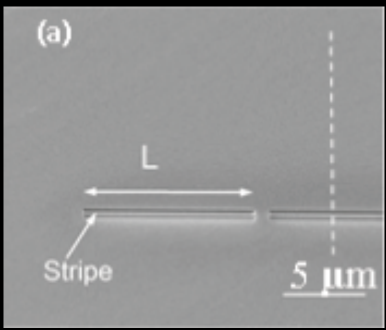

Cross sections of the center pile in stripe structure

before irr. after irr.

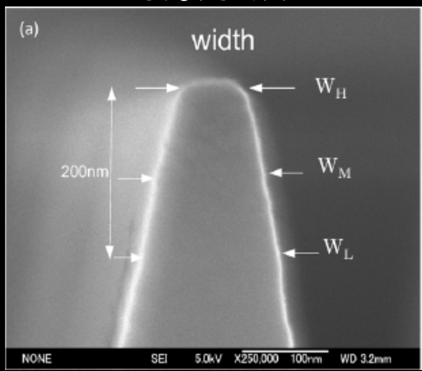

Remarkable expansion along lateral direction

Lateral deformation

Fluence and size dependences

Kr (240 keV) on c-Si with stripe structures

n ~ 8×10^{13} /cm^2

Fluence dependence

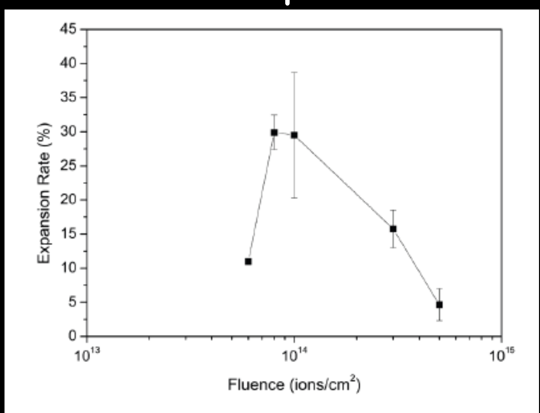

Size dependence

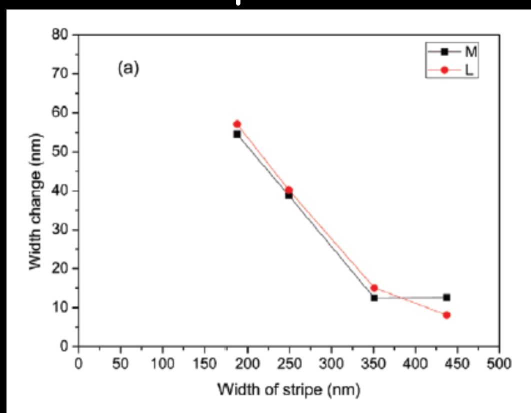

1. Max. lateral expansion is observed at n~10^{14} /cm^2.
2. Lateral expansion is suppressed for large size structure.

Lateral deformation

Shrinkage of nano-cavities : 1

As (300 keV) on a-Si with nano-cavities

M.-O. Ruault et al. Appl. Phys. Lett. 81 (2002) 2617.

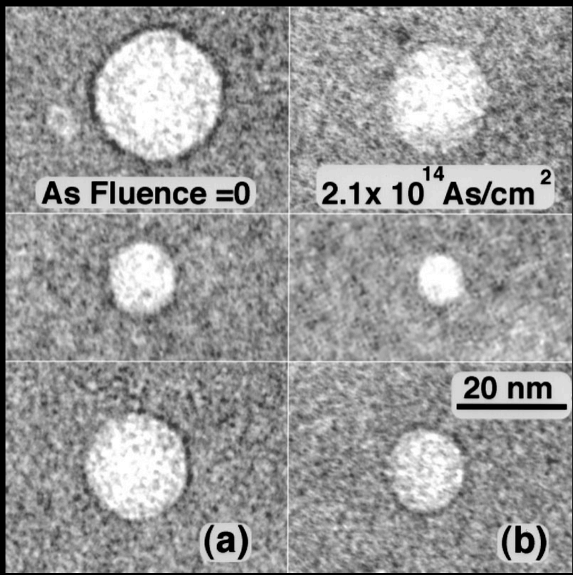

Remarkable shrinkage of nano-cavities (10~20nm)

Lateral deformation

Shrinkage of nano-cavities : 2

Kr (240 keV) on c-Si with nanocavities

n ~ 8×10^{13} /cm^2

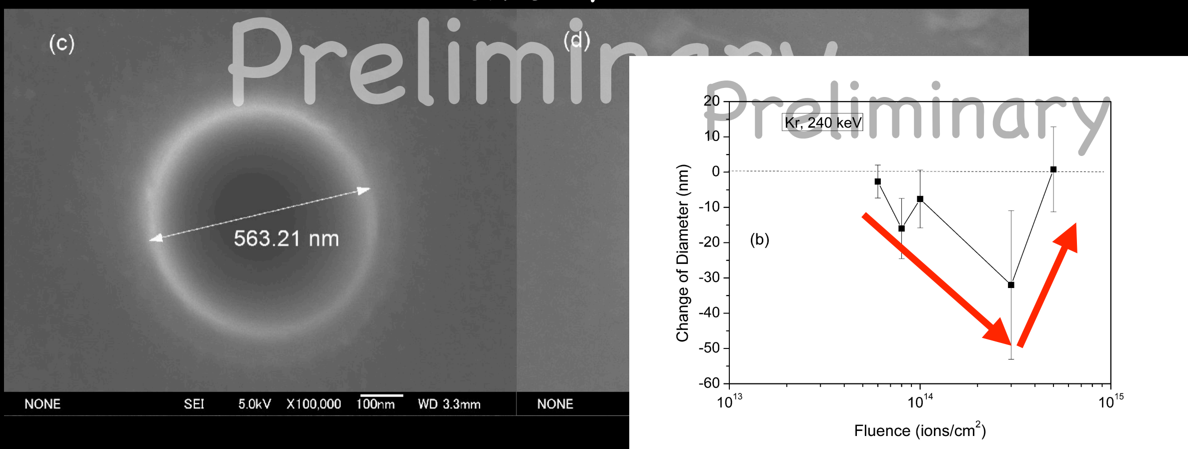

1. Max. shrinkage is observed at n~3×10^{14} /cm^2.
2. Shrinkage is suppressed at higher fluence.

What does the suppression effect at higher fluence region mean?

→ Microscopic/macroscopic observation of IB-induced defects

IB-induced defects in c-Si

Analysis of RAMAN spectrum

Accumulation of defects -> amorphous
Amorphous fraction obtained from RAMAN spectrum

X. Guo et al. e-J. Surf. Sci. Nanotech. 13 (2015) 35.

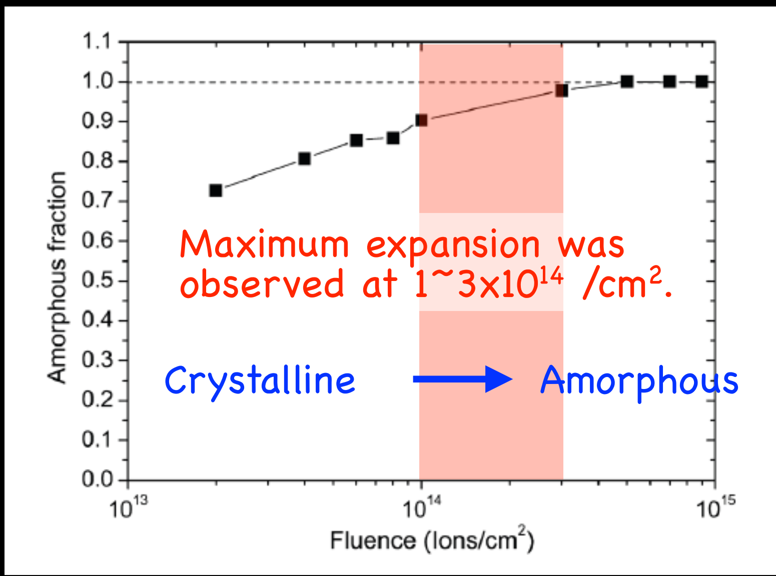

What happens at the transitional phase ?

IB-induced defects in c-Si

TEM observation

Cross-sectional TEM images of stripe structures

X. Guo et al., e-J. Surf. Sci. Nanotech. 13 (2015) 35.

n ~ 1x10^{14} /cm^2

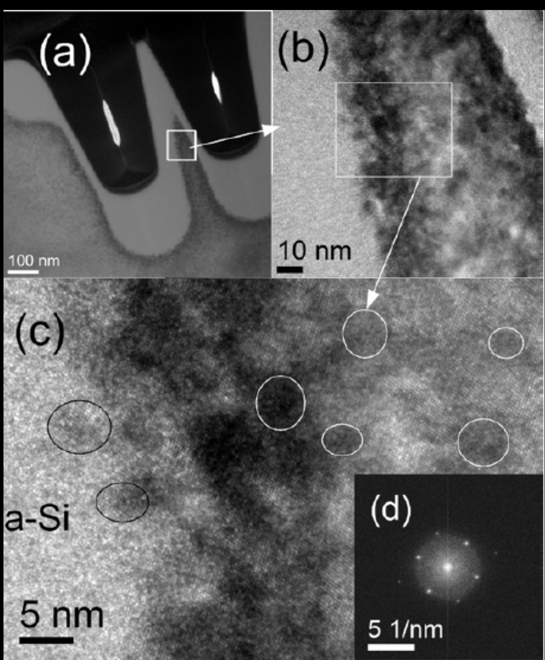

Inhomogeneous defect distribution around a boundary between c-Si and a-Si region
→ Amorphous/crystal pockets

At low fluence, defects are trapped at surfaces of a/c pockets.
→ Expansion effect enhances.

At higher fluence, trapping effect is suppressed.
→ Expansion effect decreases.
$\rho_a \sim \rho_c$

Measurement of mech. properties

Indentation method

Nano Indenter XP/DCM (Agilent Technology)

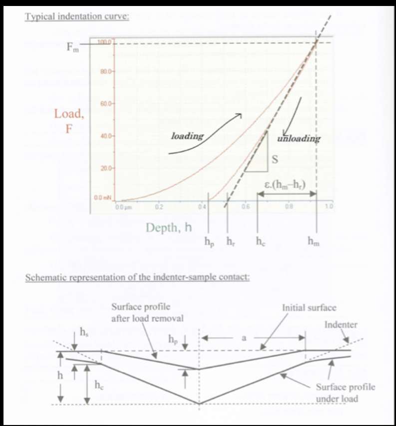

Depth profile of mechanical properties

because irradiation effect is depth dependent. However,

Conventional method :

Measurement at fixed depth

Advanced method :

Continuous measurements by means of dynamic technique

W.C. Oliver et al., J. Mat. Res. 7 (1992) 1564.

Depth profile of mech. properties

Depth-dependent mechanical properties obtained from indentation method X. Guo et al., Appl. Surf. Sci., 349 (2015) 123.

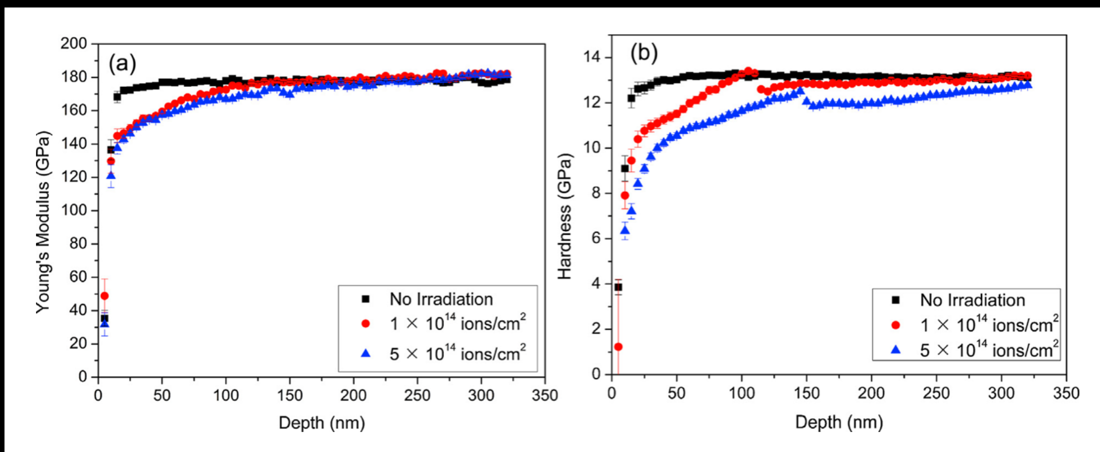

For virgin samples, consistent with conventional values

Young's modulus = 176 GPa / Hardness = 13.0 GPa

IB-induced deterioration in mechanical properties is relatively small at n~10^{14} ion/cm^2.

Comparison with TEM, RBS-c results

Depth-dependent mechanical properties obtained from indentation method X. Guo et al., Appl. Surf. Sci., 349 (2015) 123.

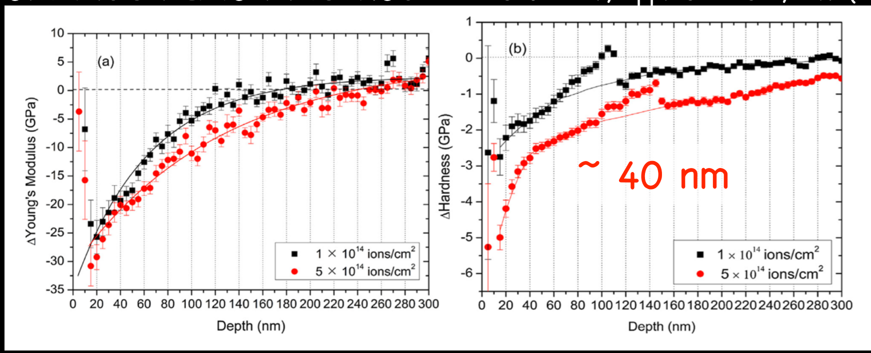

Cross-sectional TEM images

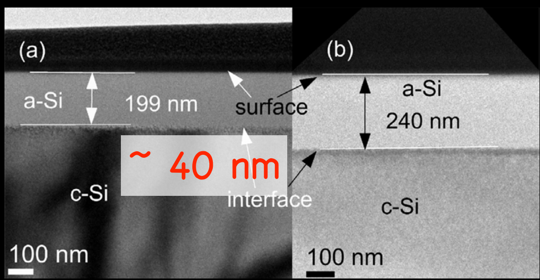

Defect distributions obtained from c-RBS measurements

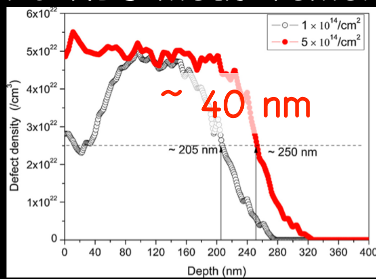

Indentation-induced phase transition

Phase transition in a-Si induced by indentation

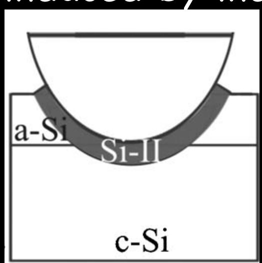

B. Haberl et al.
J. Appl. Phys., 100 (2006) 013520.

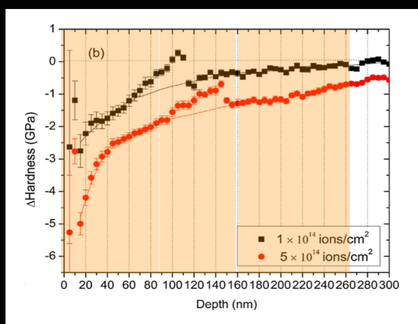

Evolution of phase transition according to indentation

Accumulation of internal stress to increase mech. prop.

Overcoming barrier and penetrate into c-region

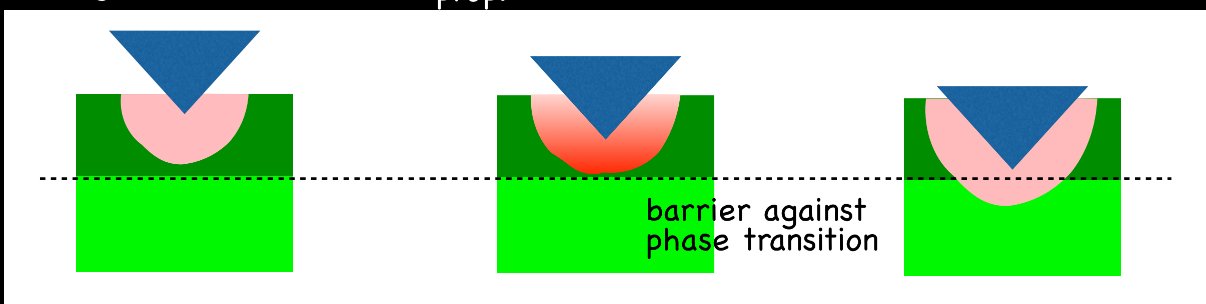

S. Momota / **Int. Conf. Appl. Eng. Phys. Sep./13-16/2015 Hanoi, Vietnam**

Conclusions

IB-induced expansion effect

Feasibility of IB-induced expansion effect as fabrication method for 3D-micro-nano scale structures

1. Control of swelling & lateral deformation on crystal materials was achieved by irradiating IB with relatively low fluence.
2. Small deterioration in mechanical properties without post-treatment was confirmed.

Behaviors of defects induce by IB irradiation

1. Inhomogeneous defect distribution would play an important role in IB-induced expansion effect on crystal.
2. Evolutional behavior of indentation-induced phase transition is found in depth-dependent indentation measurements.

Acknowledgements

Tokyo Univ. of Science :
J. Taniguchi, S. Satake

Chiva Univ. :
N. Morita

Kochi Univ. of Tech. :
N. Nitta,
J. Zhang, X. Guo, and other Lab. members

This work was supported by JSPS KAKENHI Grant-in-Aid for Scientific Research(C), Number 25420061